Unsteady Three-Dimensional Flow in a Second-Grade Fluid Over a Stretching Surface

Tasawar Hayat[a,b], Ambreen Safdar[a], Muhammad Awais[a], and Awatif A. Hendi[b]

[a] Department of Mathematics, Quaid-I-Azam University 45320, Islamabad 44000, Pakistan
[b] Department of Physics, Faculty of Sciences, King Saud University, P.O. Box 1846, Riyadh 11321, Saudi Arabia

Reprint requests to T. H.; Tel.: +92 51 90642172; E-mail: pensy_t@yahoo.com

Z. Naturforsch. **66a,** 635 – 642 (2011) / DOI: 10.5560/ZNA.2011-0032
Received April 6, 2011 / revised July 12, 2011

The three-dimensional unsteady flow induced in a second-grade fluid over a stretching surface has been investigated. Nonlinear partial differential equations are reduced into a system of ordinary differential equations by using the similarity transformations. The homotopy analysis method (HAM) has been implemented for the series solutions. Graphs are displayed for the effects of different parameters on the velocity field.

Key words: Unsteady Flow; Second-Grade Fluid; Homotopy Solution.

1. Introduction

The advancements in the flows of non-Newtonian fluids have been significantly increased in spite of their numerous applications in various fields of science and engineering. Some applications include oil and gas well drilling, waste fluids, synthetic fibers, extrusion of molten plastic, flows of polymer solutions, polymer processing, food processing, and many others. Geophysical applications involve the ice and magma flows. Many materials such as drilling mud, clay coatings and suspensions, ketchup, toothpaste, certain oils and greases, polymer melts, clastomer, and many other emulsions have been treated as non-Newtonian fluids. The flows of such fluids are frequently encountered in biomechanics, geothermal engineering, insulation systems, ceramic processing, chromatography etc. Significant progress has been made for the flows of different viscoelastic fluids. Among these models of non-Newtonian fluids, there is a simplest subclass of viscoelastic fluids, namely the second-grade fluids. Fetecau et al. [1] presented the unsteady flow of a second grade fluid between two side walls perpendicular to a plate. Exact solutions of starting flows for a second-grade fluid in a porous medium has been reported by Khan et al. [2]. Ariel [3] examined the axisymmetric flow of a second-grade fluid past a stretching sheet. Exact solutions for steady flows of second-grade fluids have been examined by Zhang et al. [4]. Cortell [5] discussed the magnetohydrodynamic (MHD) flow and mass transfer of an electrically conducting fluid of second-grade in a porous medium over a stretching sheet with chemically reactive species. Stagnation point flow of a second-grade fluid with slip is studied by Labropulu and Li [6]. Flow due to noncoaxial rotation of a porous disk and a second-grade fluid rotating at infinity has been reported by Erdogan and Imrak [7]. Hayat and Awais [8] discussed the simultaneous effect of heat and mass transfer along with Soret and Dufours effects in time-dependent flow of a second-grade fluid. Hayat et al. [9] further discussed the effect of thermal radiation on the flow of a second-grade fluid. Cortell [10] examined the viscous dissipation and thermal radiation effects on the flow and heat transfer of a power-law fluid past an infinite porous plate.

Ever since the pioneering work of Sakiadis [11, 12], the steady two-dimensional stretching flows have been studied extensively in various ways. Such flows are vital in both viscous and non-Newtonian fluids. The specific applications of such flows include hot rolling, polymer extension, crystal growing, continuous stretching of hot films, metal spinning etc. The extensive available research on stretching flow deals with the mathematical analysis in two dimensions. However, very few researchers presented such flows in three dimensions. Ariel [13, 14] found the exact and homotopy perturbation solutions of a viscous fluid for the three-dimensional flow over a stretched surface. The magnetohydrodynamic three-dimensional viscous flow over a porous stretching surface has been presented by Hayat and Javed [15]. Xu et al. [16] analyzed the series solutions of unsteady free convection flow in the stagnation-point region of a three-dimensional body. Hayat and Awais [17] studied the three-dimensional flow of a Maxwell fluid over a stretching surface.

The aim of this paper is to venture further in the regime of three-dimensional unsteady flows over a stretching surface. A simplest second-grade fluid model has been chosen because it has a rheology difference from the Newtonian model. The article has been arranged as follows. The mathematical formulation for the unsteady three-dimensional flow in a second-grade fluid has been given in Section 2. In Section 3, the homotopy analysis method (HAM) [18–30] has been used to find the series solution. Sections 4 includes the convergence and graphical results. Final discussion of the obtained results has been presented in Section 5.

2. Problem Description

The unsteady three-dimensional flow of an incompressible second-grade fluid over a stretching surface is considered. The sheet coincides with the plane at $z = 0$, and the flow occupies the region $z > 0$. A nonconducting stretching surface generates the flow in the second-grade fluid. The Cauchy stress tensor $\mathbf{T}$ in an incompressible homogenous fluid of second-grade is related to the fluid motion in the following manner [1–9]:

$$\mathbf{T} = -p\mathbf{I} + \mu\mathbf{A}_1 + \alpha_1\mathbf{A}_2 + \alpha_2\mathbf{A}_1^2, \tag{1}$$

where p, $\mathbf{I}$, μ, α_i $(i = 1,2)$ are the pressure, identity tensor, dynamic viscosity, and material constants, respectively. The Rivlin–Ericksen tensors ($\mathbf{A}_1$ and $\mathbf{A}_2$) can be computed by the following relations:

$$\mathbf{A}_1 = \nabla\mathbf{V} + (\nabla\mathbf{V})^{\mathbf{t}}, \tag{2}$$

$$\begin{aligned}\mathbf{A}_n &= \frac{\mathrm{d}\mathbf{A}_{n-1}}{\mathrm{d}t} + \mathbf{A}_{n-1}\mathbf{L} + \mathbf{L}^{\mathbf{t}}\mathbf{A}_{n-1},\\ \mathbf{L} &= \nabla\mathbf{V}, \quad n > 1.\end{aligned} \tag{3}$$

Here ∇ is the gradient operator, $\mathbf{V}$ is the velocity field, and for thermodynamic second-grade fluid, we have

$$\mu \geq 0, \ \ \alpha_1 \geq 0, \ \ \alpha_1 + \alpha_2 = 0. \tag{4}$$

The basic equations governing the flow under consideration are

$$\nabla \cdot \mathbf{V} = \mathbf{0}, \tag{5}$$

$$\rho\frac{\mathrm{d}\mathbf{V}}{\mathrm{d}t} = \nabla \cdot \mathbf{T}. \tag{6}$$

The velocity field for three-dimensional flow is chosen as

$$\mathbf{V} = [u(x,y,z), \ \ v(x,y,z), \ \ w(x,y,z)], \tag{7}$$

The scalar forms of (5) are

$$\rho\frac{\mathrm{d}u}{\mathrm{d}t} = \frac{\partial(T_{xx})}{\partial x} + \frac{\partial(T_{xy})}{\partial y} + \frac{\partial(T_{xz})}{\partial z}, \tag{8}$$

$$\rho\frac{\mathrm{d}v}{\mathrm{d}t} = \frac{\partial(T_{yx})}{\partial x} + \frac{\partial(T_{yy})}{\partial y} + \frac{\partial(T_{yz})}{\partial z}, \tag{9}$$

$$\rho\frac{\mathrm{d}w}{\mathrm{d}t} = \frac{\partial(T_{zx})}{\partial x} + \frac{\partial(T_{zy})}{\partial y} + \frac{\partial(T_{zz})}{\partial z}, \tag{10}$$

where T_{xx}, T_{yy}, and T_{zz} are the normal stresses and T_{xy}, T_{xz}, T_{yx}, T_{yz}, T_{zx}, and T_{zy} are the shear stresses. We computed the values of these stress components through (1)–(3). Using these values of stress components and the boundary layer assumptions, we get

$$\frac{\partial u}{\partial x} + \frac{\partial v}{\partial y} + \frac{\partial w}{\partial z} = 0, \tag{11}$$

$$\begin{aligned}&\rho\left(\frac{\partial u}{\partial t} + u\frac{\partial u}{\partial x} + v\frac{\partial u}{\partial y} + w\frac{\partial u}{\partial z}\right)\\ &= \mu\frac{\partial^2 u}{\partial z^2} + \alpha_1\left(\begin{array}{c} u\dfrac{\partial^3 u}{\partial x\partial z^2} + v\dfrac{\partial^3 u}{\partial y\partial z^2} + w\dfrac{\partial^3 u}{\partial z^3}\\ -\dfrac{\partial u}{\partial z}\dfrac{\partial^2 w}{\partial z^2} + \dfrac{\partial u}{\partial x}\dfrac{\partial^2 u}{\partial z^2} + \dfrac{\partial^2 v}{\partial z\partial x}\dfrac{\partial v}{\partial z}\\ +\dfrac{\partial v}{\partial x}\dfrac{\partial^2 v}{\partial z^2} - \dfrac{\partial u}{\partial z}\dfrac{\partial^2 v}{\partial y\partial z} + \dfrac{\partial^3 u}{\partial t\partial z^2}\end{array}\right),\end{aligned} \tag{12}$$

$$\begin{aligned}&\rho\left(\frac{\partial v}{\partial t} + u\frac{\partial v}{\partial x} + v\frac{\partial v}{\partial y} + w\frac{\partial v}{\partial z}\right)\\ &= \mu\frac{\partial^2 v}{\partial z^2} + \alpha_1\left(\begin{array}{c} u\dfrac{\partial^3 v}{\partial x\partial z^2} + v\dfrac{\partial^3 v}{\partial y\partial z^2} + w\dfrac{\partial^3 v}{\partial z^3}\\ -\dfrac{\partial v}{\partial z}\dfrac{\partial^2 w}{\partial z^2} + \dfrac{\partial u}{\partial y}\dfrac{\partial^2 u}{\partial z^2} + \dfrac{\partial^2 v}{\partial z^2}\dfrac{\partial v}{\partial y}\\ +\dfrac{\partial u}{\partial z}\dfrac{\partial^2 u}{\partial y\partial z} - \dfrac{\partial v}{\partial z}\dfrac{\partial^2 u}{\partial x\partial z} + \dfrac{\partial^3 v}{\partial t\partial z^2}\end{array}\right).\end{aligned} \tag{13}$$

The subjected boundary conditions are given by

$$\begin{aligned} &u=\frac{ax}{1-ct},\ v=\frac{bx}{1-ct},\ w=0 \quad \text{at } z=0,\\ &u\to 0,\ v\to 0,\ \frac{\partial u}{\partial z}\to 0,\ \frac{\partial v}{\partial z}\to 0 \quad \text{as } z\to\infty, \end{aligned} \tag{14}$$

where u, v, and w are the velocities parallel to the x, y, and z-directions, respectively, ρ indicates the fluid density, μ the dynamic viscosity, α_1 the second-grade parameter, and $a>0$, $b>0$, and $ct<1$ are the constants. We now define

$$\begin{aligned} &\eta=\sqrt{\frac{a}{\nu(1-ct)}}z,\ u=\frac{ax}{1-ct}f'(\eta),\\ &v=\frac{ay}{1-ct}g'(\eta),\ w=-\sqrt{\frac{a\nu}{1-ct}}\ \{f(\eta)+g(\eta)\}. \end{aligned} \tag{15}$$

All the quantities appearing in (11)–(13) have been computed by using the chain rule through (15). It is noticed that (11) is identically satisfied and (12) and (13) become

$$f'''-f'^2+(f+g)f''-A\left(f'+\frac{\eta}{2}f''\right)+\alpha\left[\begin{array}{c} f''^2+2f'f'''-(f+g)f^{iv}\\ +A\left(2f'''+\frac{\eta}{2}f^{iv}\right)\end{array}\right]=0, \tag{16}$$

$$g'''-g'^2+(f+g)g''-A\left(g'+\frac{\eta}{2}g''\right)+\alpha\left[\begin{array}{c} g''^2+2g'g'''-(f+g)g^{iv}\\ +A\left(2g'''+\frac{\eta}{2}g^{iv}\right)\end{array}\right]=0. \tag{17}$$

Now the boundary conditions through (14) and (15) give

$$\begin{aligned} &f(0)=0,\ f'(0)=1,\ f'(\infty)=0,\\ &g(0)=0,\ g'(0)=p,\ g'(\infty)=0, \end{aligned} \tag{18}$$

where A is the time-dependent parameter, α is the dimensionless second-grade parameter, and p is the stretching ratio defined as

$$A=c/a,\ \alpha=\frac{\alpha_1 a}{\mu(1-ct)},\ p=b/a. \tag{19}$$

3. Series Solutions

3.1. Zeroth-Order Deformation Problems

The velocity distributions $f(\eta)$ and $g(\eta)$ in the set of base functions

$$\{\eta^k\exp(-n\eta)\mid k\geq 0, n\geq 0\} \tag{20}$$

are given by

$$f(\eta)=a_{0,0}^0+\sum_{n=0}^{\infty}\sum_{k=0}^{\infty}a_{m,n}^k\eta^k\exp(-n\eta), \tag{21}$$

$$g(\eta)=A_{0,0}^0+\sum_{n=0}^{\infty}\sum_{k=0}^{\infty}A_{m,n}^k\eta^k\exp(-n\eta), \tag{22}$$

where the initial guesses are

$$f_0(\eta)=1-\exp(-\eta), \tag{23}$$

$$g_0(\eta)=p(1-\exp(-\eta)). \tag{24}$$

The linear operators and their associated properties are

$$\mathcal{L}_f=\frac{\mathrm{d}^3f}{\mathrm{d}\eta^3}-\frac{\mathrm{d}f}{\mathrm{d}\eta}, \tag{25}$$

$$\mathcal{L}_g=\frac{\mathrm{d}^3g}{\mathrm{d}\eta^3}-\frac{\mathrm{d}g}{\mathrm{d}\eta}, \tag{26}$$

$$\mathcal{L}_f\left[C_1+C_2\exp(\eta)+C_3\exp(-\eta)\right]=0, \tag{27}$$

$$\mathcal{L}_g\left[C_4+C_5\exp(\eta)+C_6\exp(-\eta)\right]=0, \tag{28}$$

where C_1-C_6 are constants and $a_{m,n}^k$ and $A_{m,n}^k$ are coefficients.

The problems corresponding to the zeroth-order deformation can be written as

$$\begin{aligned} &(1-p)\mathcal{L}\left[\bar f(\eta,p)-f_0(\eta)\right]\\ &\qquad=p\hbar_f\mathcal{N}_f[\bar f(\eta,p),\bar g(\eta,p)], \end{aligned} \tag{29}$$

$$\begin{aligned} &(1-p)\mathcal{L}\left[\bar g(\eta,p)-g_0(\eta)\right]\\ &\qquad=p\hbar_g\mathcal{N}_g[\bar f(\eta,p),\bar g(\eta,p)], \end{aligned} \tag{30}$$

$$\begin{aligned} &\bar f(0,p)=0,\ \bar f'(0,p)=1,\ \bar g(0,p)=0,\\ &\bar g'(0,p)=p,\ \bar f'(\infty,p)=0,\ \bar g'(\infty,p)=0, \end{aligned} \tag{31}$$

$$\begin{aligned}\mathcal{N}_f[\bar{f}(\eta,p),\bar{g}(\eta,p)] &= \frac{\partial^3\bar{f}}{\partial\eta^3}-\left(\frac{\partial\bar{f}}{\partial\eta}\right)^2\\ &+\{\bar{f}(\eta,p)+\bar{g}(\eta,p)\}\frac{\partial^2\bar{f}}{\partial\eta^2}\\ &-A\left\{\bar{f}'(\eta,p)+\frac{\eta}{2}\bar{f}''(\eta,p)\right\}\\ &+\alpha\left[\begin{array}{c}\bar{f}''^2(\eta,p)+2\bar{f}'(\eta,p)\bar{f}'''(\eta,p)\\ -\{\bar{f}(\eta,p)+\bar{g}(\eta,p)\}\bar{f}^{iv}(\eta,p)\\ +A\{2\bar{f}'''(\eta,p)+\frac{\eta}{2}\bar{f}^{iv}(\eta,p)\}\end{array}\right],\end{aligned} \tag{32}$$

$$\begin{aligned}\mathcal{N}_g[\bar{f}(\eta,p),\bar{g}(\eta,p)] &= \frac{\partial^3\bar{g}}{\partial\eta^3}-\left(\frac{\partial\bar{g}}{\partial\eta}\right)^2\\ &+\{\bar{f}(\eta,p)+\bar{g}(\eta,p)\}\frac{\partial^2\bar{g}}{\partial\eta^2}\\ &-A\left\{\bar{g}'(\eta,p)+\frac{\eta}{2}\bar{g}''(\eta,p)\right\}\\ &+\alpha\left[\begin{array}{c}\bar{g}''^2(\eta,p)+2\bar{g}'(\eta,p)\bar{g}'''(\eta,p)\\ -\{\bar{f}(\eta,p)+\bar{g}(\eta,p)\}\bar{g}^{iv}(\eta,p)\\ +A\{2\bar{g}'''(\eta,p)+\frac{\eta}{2}\bar{g}^{iv}(\eta,p)\}\end{array}\right].\end{aligned} \tag{33}$$

Here $\hbar_f$ and $\hbar_g$ show the auxiliary non-zero parameters and $p\in[0,1]$ indicates an embedding parameter. We have for $p=0$ and $p=1$

$$\begin{aligned}\bar{f}(\eta,0)&=f_0(\eta), & \bar{f}(\eta,1)&=f(\eta),\\ \bar{g}(\eta,0)&=g_0(\eta), & \bar{g}(\eta,1)&=g(\eta),\end{aligned} \tag{34}$$

and the initial guesses $f_0(\eta)$ and $g_0(\eta)$ approach to the final solutions $f(\eta)$ and $g(\eta)$ when p varies from 0 to 1. In view of Taylor's expression

$$\bar{f}(\eta,p)=f_0(\eta)+\sum_{m=1}^{\infty}f_m(\eta)p^m, \tag{35}$$

$$\bar{g}(\eta,p)=g_0(\eta)+\sum_{m=1}^{\infty}g_m(\eta)p^m, \tag{36}$$

$$\begin{aligned}f_m(\eta)&=\frac{1}{m!}\frac{\partial^m\bar{f}(\eta,p)}{\partial p^m}\bigg|_{p=0},\\ g_m(\eta)&=\frac{1}{m!}\frac{\partial^m\bar{g}(\eta,p)}{\partial p^m}\bigg|_{p=0},\end{aligned} \tag{37}$$

the convergence of series (35) and (36) depends upon $\hbar_f$ and $\hbar_g$. $\hbar_f$ and $\hbar_g$ are chosen in such a way that the series (35) and (36) converge for $p=1$. Hence,

$$f(\eta)=f_0(\eta)+\sum_{m=1}^{\infty}f_m(\eta), \tag{38}$$

$$g(\eta)=g_0(\eta)+\sum_{m=1}^{\infty}g_m(\eta). \tag{39}$$

3.2. mth-Order Deformation Problems

The problems corresponding to the mth-order deformations are

$$\mathcal{L}_f\left[f_m(\eta)-\chi_m f_{m-1}(\eta)\right]=\hbar_f\mathcal{R}_{f,m}(\eta), \tag{40}$$

$$\mathcal{L}_g\left[g_m(\eta)-\chi_m g_{m-1}(\eta)\right]=\hbar_g\mathcal{R}_{g,m}(\eta), \tag{41}$$

$$\begin{aligned}f_m(0)&=f'_m(0)=f'_m(\infty)=g_m(0)\\ &=g'_m(0)=g'_m(\infty)=0,\end{aligned} \tag{42}$$

$$\begin{aligned}\mathcal{R}_m^f(\eta)=&f'''_{m-1}+\sum_{k=0}^{m-1}\left[(f_{m-1-k}+g_{m-1-k})f''_k-f'_{m-1-k}f'_k\right]-A\left(f'_{m-1}+\frac{\eta}{2}f''_{m-1}\right)\\ &+\alpha\left[\begin{array}{c}\sum_{k=o}^{m-1}\{f''_{m-1-k}f''_k+2f'_{m-1-k}f'''_k-(f_{m-1-k}+g_{m-1-k})f_k^{iv}\}\\ +A\left(2f'''_{m-1}+\frac{\eta}{2}f^{iv}_{m-1}\right)\end{array}\right],\end{aligned} \tag{43}$$

$$\begin{aligned}\mathcal{R}_m^g(\eta)=&g'''_{m-1}+\sum_{k=0}^{m-1}\left[(f_{m-1-k}+g_{m-1-k})g''_k-g'_{m-1-k}g'_k\right]-A\left(g'_{m-1}+\frac{\eta}{2}g''_{m-1}\right)\\ &+\alpha\left[\begin{array}{c}\sum_{k=o}^{m-1}\{g''_{m-1-k}g''_k+2g'_{m-1-k}g'''_k-(f_{m-1-k}+g_{m-1-k})g_k^{iv}\}\\ +A\left(2g'''_{m-1}+\frac{\eta}{2}g^{iv}_{m-1}\right)\end{array}\right],\end{aligned} \tag{44}$$

$$\chi_m = \begin{cases} 0, & m \le 1 \\ 1, & m > 1 \end{cases}. \tag{45}$$

Upon using Mathematica, the resulting problems for $m = 1, 2, 3, \ldots$ have been solved successfully.

It is worth mentioning to point out that the present problem for $A = 0 = \alpha$ reduces to the problem of a viscous fluid. Exact numerical solution for this viscous fluid problem is computed by Ariel [13]. He employed the Ackroyd method for solving the arising mathematical problem. For details of this Ackroyd method one may consult [13]. The present attempt extends the analysis of Ariel [13] from viscous to second-grade fluid. The considered fluid model is prefered in the sense that it can easily describe the normal stress effects. This consideration hikes the order of the differential system. Further, the governing equations are more complicated and nonlinear. Such complexities appear due to viscoelastic properties of the second-grade fluid. Another difference occurs in the boundary conditions. Ariel [13] considered the steady case of stretching surface whereas unsteady stretched flow is taken into account in the present analysis. A recent and quite popular technique, namely the homotopy analysis method, is used for the solution of the highly nonlinear problem.

4. Convergence of the Series Solutions

It is noted that the convergence of the solution depends on $\hbar_f$ and $\hbar_g$. Figure 1 helps for the allowed values of $\hbar_f$ and $\hbar_g$ for the convergent solutions. This figure shows that admissible values are $-1 \le (\hbar_f, \hbar_g) \le -0.25$. Table 1 is presented to find the necessary order of approximation for a convergent solution. It is noticed that 20th-order approximations are sufficient. Table 2 is displayed in order to provide a comparative study for a limiting case. The conclusions show that present results are in a very good agreement with the previous limiting results found by Ariel [13, 14]

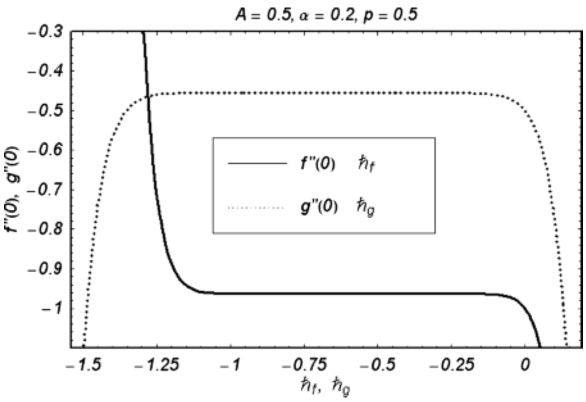

Fig. 1. h-curves of f and g for the 15th order of approximation.

Table 1. Convergence of the HAM solutions for different order of approximations when $p = 0.5$, $\alpha = 0.2$, $A = 0.5$.

order of approximation	$-f''(0)$	$-g''(0)$
1	0.953333	0.453333
2	0.965036	0.455542
5	0.455542	0.455301
10	0.455301	0.455231
15	0.962639	0.455227
20	0.962639	0.455226
25	0.962639	0.455226
30	0.962639	0.455226
40	0.962639	0.455226
50	0.962639	0.455226

Table 2. Illustrating the variation of $-f''(0)$ and $-g''(0)$ with p when $A = 0 = \alpha$, using HAM, HPM (Ariel [13, 14]), and the exact solution (Ariel [13, 14]).

p		$-f''(0)$			$-g''(0)$	
	HAM	HPM [13, 14]	Exact [13, 14]	HAM	HPM [13, 14]	Exact [13, 14]
0.0	1	1	1	0	0	0
0.1	1.020259	1.017027	1.020259	0.066847	0.073099	0.066847
0.2	1.039495	1.034587	1.039495	0.148736	0.158231	0.148736
0.3	1.057954	1.052470	1.057954	0.243359	0.254347	0.243359
0.4	1.075788	1.070529	1.075788	0.349208	0.360599	0.349208
0.5	1.093095	1.088662	1.093095	0.465204	0.476290	0.465204
0.6	1.109946	1.106797	1.109946	0.590528	0.600833	0.590528
0.7	1.126397	1.124882	1.126397	0.724531	0.733730	0.724531
0.8	1.142488	1.142879	1.142488	0.866682	0.874551	0.866682
0.9	1.158253	1.160762	1.158253	1.016538	1.022922	1.016538
1.0	1.173720	1.178511	1.173720	1.173720	1.178511	1.173720

5. Results and Discussion

In this section the behaviour of certain parameters of interest on the velocity field has been analyzed. Figures 2 – 9 are plotted for this interest. The variations of A on f' and g' are shown in Figures 2 – 5. The effects of the time-dependent parameter A on f' for two-dimensional flow are presented in Figure 2. It shows that f' and the associated boundary layer is an increasing function of A. Figures 3 and 4 also show the

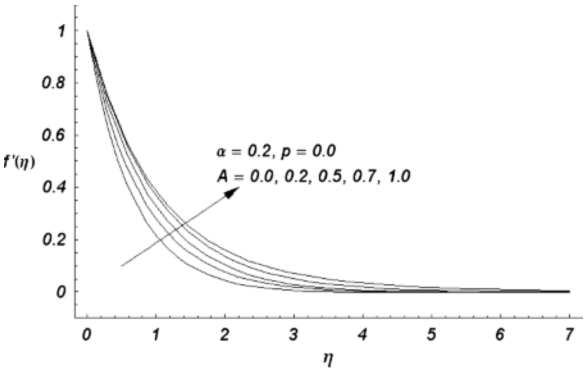

Fig. 2. Influence of A on f' for two-dimensional flow.

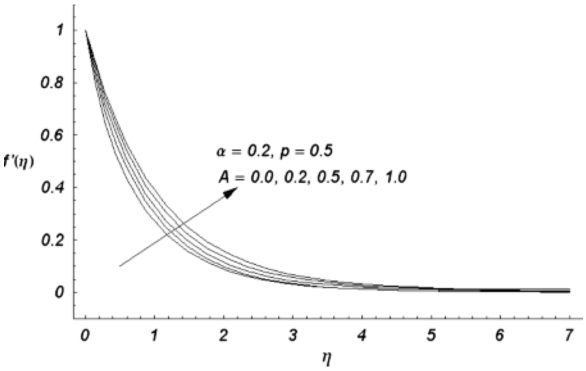

Fig. 3. Influence of A on f' for three-dimensional flow.

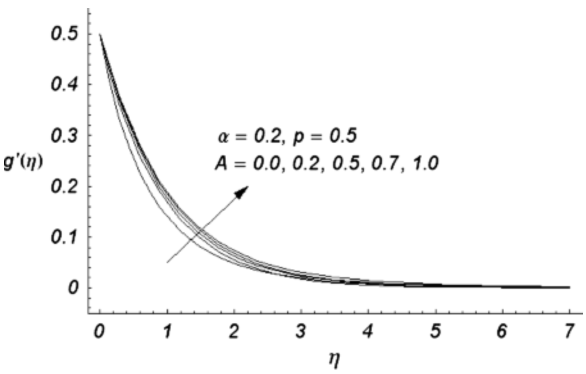

Fig. 4. Influence of A on g' for three-dimensional flow.

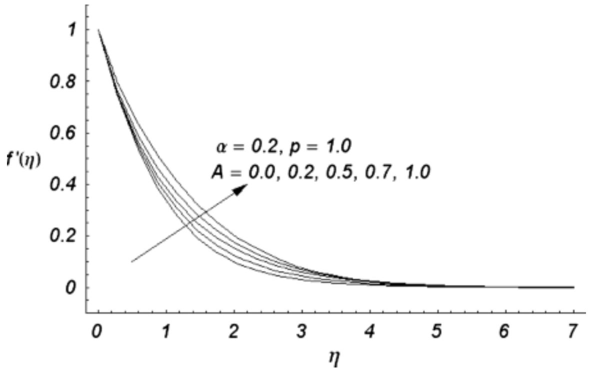

Fig. 5. Influence of A on f' for axisymmetric flow.

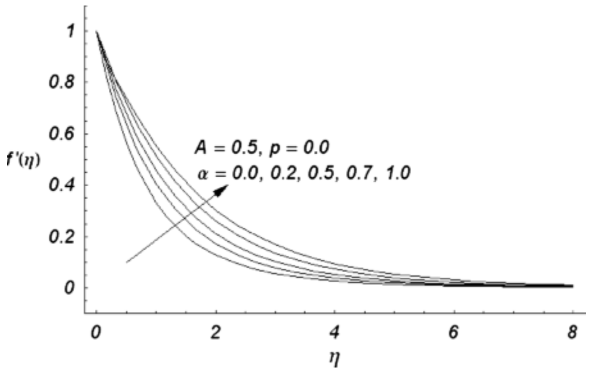

Fig. 6. Influence of α on f' for two-dimensional flow.

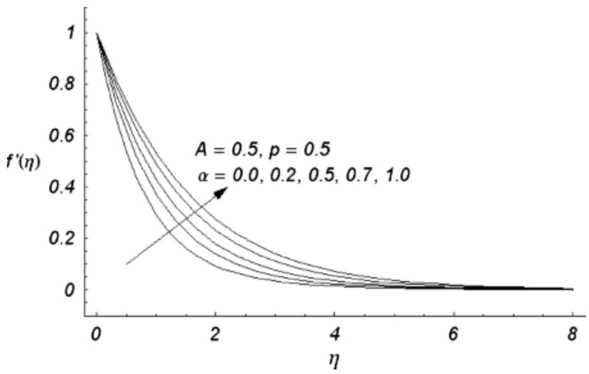

Fig. 7. Influence of α on f' for three-dimensional flow.

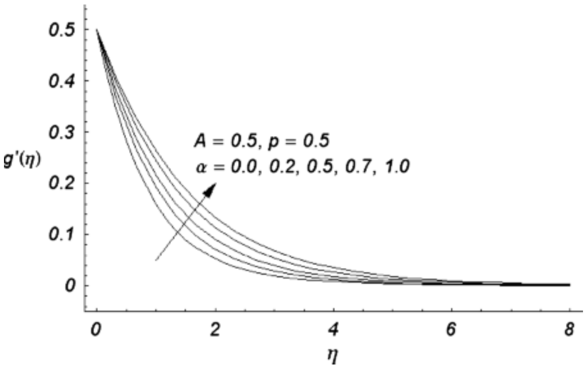

Fig. 8. Influence of α on g' for three-dimensional flow.

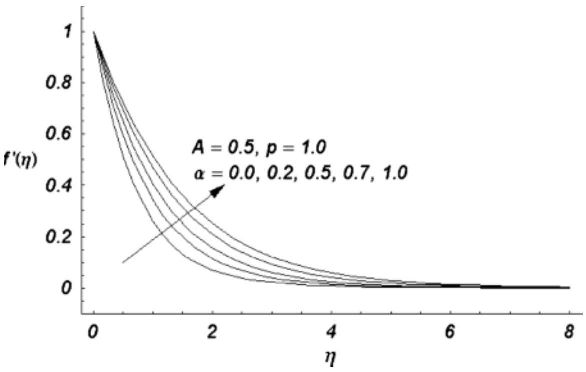

Fig. 9. Influence of α on f' for axisymmetric flow.

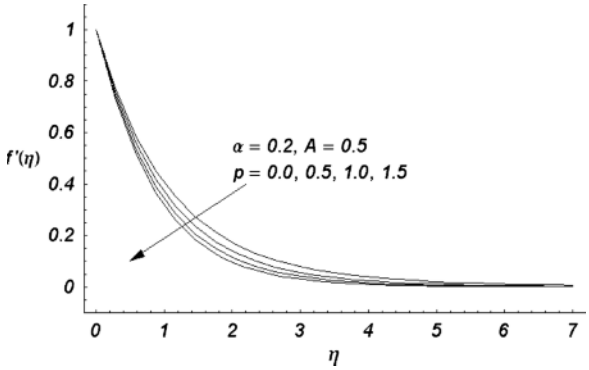

Fig. 10. Influence of p on f'.

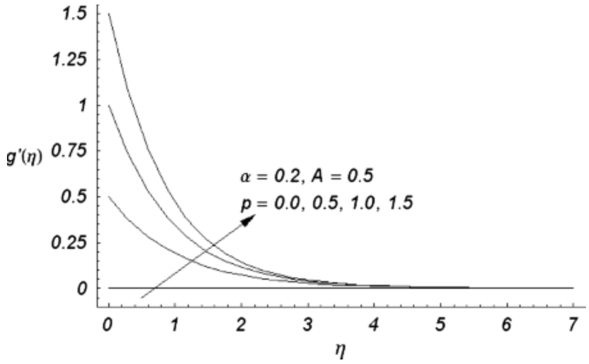

Fig. 11. Influence of p on g'.

increasing behaviour of A on f' and g' for the three-dimensional flow. From Figure 5 it is observed that similar result is obtained for axisymmetric flow.

The effects of the second-grade parameter α on f' and g' are displayed in Figures 6 – 9. Figure 6 elucidates that f' and the associate boundary layer isan increasing function of α. Similar results are obtained from Figures 7 and 8 for the three-dimensional flow. Figure 9 represents increasing effects of α on f' for the axisymmetric flow. Figure 10 illustrates the variation of p on f'. This figure indicates that the velocity field f' and the boundary layer thickness decreases with an increase in p. Figure 11 analyzes the effects of p on g'. This figure shows that the velocity component g' increases with an increase in p.

Acknowledgement

The first author as a visiting professor thanks the partial support of Global Research Network for Computational Mathematics and King Saud University for this research.

[1] C. Fetecau, T. Hayat, C. Fetecau, and N. Ali, Nonlin. Analysis: Real World Appl. **9**, 1236 (2008).
[2] M. Khan, E. Naheed, C. Fetecau, and T. Hayat, Int. J. Nonlin. Mech. **43**, 868 (2008).
[3] P. D. Ariel, Int. J. Eng. Sci. **39**, 529 (2001).
[4] D. X. Zhang, S. X. Feng, Z. M. Lu, and Y. L. Liu, J. Shanghai Uni., **13**, 340 (2009).
[5] R. Cortell, Chem. Eng. Processing **46**, 721 (2007).
[6] F. Labropulu and D. Li, Int. J. Nonlin. Mech. **43**, 941 (2008).
[7] M. E. Erdogan and C. E. Imrak, Int. J. Nonlin. Mech. **46**, 986 (2011).
[8] T. Hayat and M. Awais, Int. J. Numer. Meth. Fluids, Doi: 10.1002/fld.2414 (2011).
[9] T. Hayat, M. Nawaz, M. Sajid, and S. Asghar, Comp. Math. Appl. **58**, 369 (2009).

[10] R. Cortell, Chem. Eng. Research Design **89**, 85 (2011).
[11] B. C. Sakiadis, AIChE J. **7**, 26 (1961).
[12] B. C. Sakiadis, AIChE J. **7**, 221 (1961).
[13] P. D. Ariel, Z. Angew. Math. Mech. **83**, 844 (2003).
[14] P. D. Ariel, Comp. Math. Appl. **54**, 920 (2007).
[15] T. Hayat and T. Javed, Phys. Lett. A **370**, 243 (2007).
[16] H. Xu, S. J. Liao, and I. Pop, Int. J. Thermal Sci. **47**, 600 (2008).
[17] T. Hayat and M. Awais, Int. J. Numer. Meth. Fluids **66**, 875 (2011).
[18] S. J. Liao, Int. J. Heat Mass Transfer **48**, 2529 (2005).
[19] N. Konsar and S. J. Liao, Nonlin. Analysis: Real World Appl. **12**, 333 (2011).
[20] S. Abbasbandy and E. Shivanian, Commun. Nonlin. Sci. Numer. Simul. **15**, 3830 (2010).
[21] S. Abbasbandy, E. Shivanian, and K. Vajravelu, Commun. Nonlin. Sci. Numer. Simul. **16**, 4268 (2011).
[22] A. S. Bataineh, M. S. M. Noorani, and I. Hashim, Phys. Lett. A **372**, 4062 (2008).
[23] A. S. Bataineh, M. S. M. Noorani, and I. Hashim, Commun. Nonlin. Sci. Numer. Simul. **14**, 430 (2009).
[24] B. Sahoo, Commun. Nonlin. Sci. Numer. Simul. **15**, 602 (2010).
[25] C. Y. Cheng, Int. Commun. Heat Mass Transfer **36**, 1020 (2009).
[26] T. Hayat, M. Awais, S. Asghar, and A. A. Hendi, ASME, J. Fluid Eng. **133**, 061201 (2011).
[27] T. Hayat, S. Iram, T. Javed, and S Asghar, Z. Naturforsch. **65a**, 45 (2010).
[28] T. Hayat, M. Nawaz, and Awatif A. Hendi, Z. Naturforsch. **66a**, 53 (2011).
[29] T. Hayat, M. Qasim, and Z. Abbas, Z. Naturforsch. **65a**, 231 (2010).
[30] T. Hayat, M. Awais, M. Qasim, and A. A. Hendi, Int. J. Heat Mass Transfer **54**, 3777 (2011).